2008

In-Situ Measurement of Absorption Rates in Horizontal-Tube Falling-Film Ammonia-Water Absorbers: Part II – Heat and Mass Transfer Coefficients

Sangsoo Lee
Samsung Techwin

Lalit Kumar Bohra
ExxonMobil

Srinivas Garimella
Georgia Institute of Technology

In-situ Measurement of Absorption Rates in Horizontal-Tube Falling-Film Ammonia-Water Absorbers: Part II – Heat and Mass Transfer Coefficients

Sangsoo LEE[1], Lalit Kumar BOHRA[2], Srinivas GARIMELLA[3*]

[1]Samsung Techwin, Power Systems Department
Changwon City, South Korea
Phone : 010-8399-0543 ; E-mail: moonsign@gmail.com

[2]ExxonMobil Upstream Research Company, Gas & Facilities Division
Houston, TX, USA
Phone: (713) 431-7852; Email: lalit.bohra@exxonmobil.com

[3]Georgia Institute of Technology, GWW School of Mechanical Engineering
Atlanta, GA 30332, USA
Phone: (404) 894-7479; E-mail: srinivas.garimella@me.gatech.edu

*Corresponding Author

ABSTRACT

An experimental investigation of heat and mass transfer in a horizontal-tube falling-film ammonia-water absorber was conducted. A tube bank consisting of four columns of six 9.5 mm nominal OD, 0.292 m long tubes was installed in an absorber shell that allowed heat and mass transfer measurements and optical access for flow visualization. This absorber was installed in a test facility consisting of all the components of a functional absorption chiller, which was fabricated to obtain realistic operating conditions at the absorber to account for the influence of the other components in the system. Tests were conducted over a wide range of operating conditions (nominally, desorber solution outlet concentrations of 5 - 40% for three nominal absorber pressures of 150, 345 and 500 kPa, over solution flow rates of 0.019 – 0.034 kg/s.) The development of the test facility, and the measurement and analysis techniques were discussed in the companion paper (Part I). Results, including the component level heat transfer rates, and solution- and vapor-side heat and mass transfer coefficients, are discussed in this paper. The effects of solution flow rate, concentration, and pressure on heat and mass transfer coefficients are discussed.

1. INTRODUCTION

In an absorption heat pump, the absorber, in which refrigerant vapor is absorbed into the dilute solution with the release of a substantial amount of heat of absorption, governs the viability of the entire cycle and has been referred to as the "bottleneck" (Beutler *et al.* 1996). However, a lack of understanding of this inherently complicated process has led to the use of poor designs employing inappropriate and oversized heat and mass exchangers. The ammonia-water fluid pair has a volatile absorbent, thus presenting both heat and mass transfer resistances across the respective temperature and concentration gradients in both the liquid and vapor phases. The highly non-ideal ammonia-water fluid pair releases a considerable amount of heat of absorption at the vapor-liquid interface that must be transferred across a liquid film into the coolant. Absorption is governed by liquid and vapor phase saturation conditions, operating pressures and component geometry. The various driving potentials and local gradients in these phases can be quite different at conditions close to saturation and those that involve subcooling of the incoming liquid solution. The inlet subcooling characteristic of the dilute solution entering an absorber that is part of an operational heat pump system introduces considerable confounding influences that make it challenging to isolate the contribution, to absorption, of the corresponding equilibrium conditions, and those due to the subcooling. The coupled heat and mass transfer processes in both phases have presented challenges for analysis, modeling, experimental validation, and design. In addition, the fluid flow in the respective phases is rarely well defined (as a smooth, laminar film, for

example) (Killion and Garimella 2003a). Critical reviews of absorption heat and mass transfer models (Killion and Garimella 2001) and experiments (Killion and Garimella 2003b) are available in the literature. These reviews have pointed out that research on ammonia-water absorption has often resulted in seemingly conflicting conclusions about the governing transfer resistances, although further analysis could show that the conclusions are not so much conflicting as being limited in the extent of their applicability. Any of a number of transport operations may control the absorption process, with different resistances being dominant in different regions and for different conditions.

2. EXPERIMENTS AND ANALYSES SUMMARY

The present work recognizes that most of the available experimental studies were conducted at conditions (solution and vapor concentrations and operating pressures) totally unlike those encountered in operating absorption systems. Also, prior studies were conducted on single-pressure component test facilities that include only the absorber, solution heat exchanger, and desorber, which also provide unrealistic and very limited ranges of conditions at the absorber. Therefore, this study investigates heat and mass transfer phenomena in an ammonia-water absorber of a representative geometry operating in a test facility replicating a single-stage absorption heat pump. The test facility, which includes principally an absorber, desorber, separator, rectifier, condenser, evaporator, pre-cooler, solution heat exchanger, and the respective fluid loops coupling the components to the respective heat sources or sinks, was described in detail in Part I. The horizontal-tube falling-film absorber tube array is housed in a 0.5 m long × 0.30 m diameter outer shell with a large 0.27 m port, and three additional 64 mm sight ports for illumination and viewing at other angles. The tube array inside the shell consists of four columns of 9.5 mm OD, 0.7 mm wall thickness, 0.29 m long tubes, each column containing 6 tubes, for a total of 24 tubes in the bundle. The tubes are arranged in a serpentine configuration with a horizontal pitch of 30 mm, a vertical pitch of 20 mm, and a surface area of 0.210 m^2. The two absorber coolant headers at either side of the tube array allow serpentine flow configuration for the coolant. Dilute solution is introduced on to the tube bundle from a drip tray with capillary tubes above the tube bundle. Additional details about the test facility and the experimental procedures are available in Part I, and also in Lee (2007) and Bohra (2007). Testing was conducted at nominal absorber pressures of 150, 345 and 500 kPa, with nominal desorber outlet concentrations of 5, 15, 25, and 40%. Also, at each of these combinations of conditions, tests were conducted for three solution flow rates, 0.019, 0.026, and 0.034 kg/s.

State points at each location in the test facility were obtained from measured temperatures and pressures, and either the appropriate quality, or the concentration obtained from mass and species balances. Other properties such as enthalpy and specific volume were obtained using these three known independent parameters. (In some instances, the enthalpy obtained from energy balances is used as an input to compute quality or concentration.) At the absorber, measured mass flow rates and calculated enthalpies of the three working fluid streams are used to calculate the solution-side heat duty. The coolant-side heat duty is calculated using the absorber coolant flow rate and temperatures at the inlet and outlet. In the entire data set of 36 points, 20 showed energy balances within 5%, 14 points within 10%, and 2 points within 15%, for an average absolute deviation of 4.77%. Energy balances were established not just at the absorber, but also for each component in the system, which is important because flow rates and concentrations at the absorber, depend to a large extent on system-wide state points.

To compute the overall heat transfer coefficient *UA* from the measured flow rates, an *LMTD* based on the measured (rather than saturation) solution and coolant temperatures in the absorber was used. This definition accounts for the fact that in the tests conducted in this system-level facility, an idealized driving temperature difference based on saturation temperatures is inadequate for heat transfer in the absorption process because the bulk solution is significantly subcooled throughout the absorber. The solution heat transfer coefficient was obtained from the measured overall *UA* using a thermal resistance network analysis.

Coupled heat and mass transfer analyses were conducted to evaluate the absorption of refrigerant and absorbent from the bulk vapor to the interface and from the interface to the bulk liquid. The bulk vapor was assumed to achieve conditions corresponding to saturation at the minimum temperature in the absorber (solution pool or exit of tube array) and the average absorber pressure upon entry into the absorption chamber. Vapor sensible cooling or heating between the vapor bulk and the interface, latent heat release at the interface, condensed vapor sensible cooling from the interface to the solution bulk, solution sub-cooling were computed. Interface conditions were taken as those of saturation at the solution bulk temperature and absorber pressure, unlike much of the literature, where the interface conditions are assumed to be those corresponding to saturated liquid at the solution bulk concentration (assuming complete mixing in the solution). The heat duties of the phase-change at the interface and

of the subsequent sub-cooling of the solution are the largest contributors to the overall duty removed by the coolant. The latent heat duty is used for determining the condensing flux concentration z by equating the latent heat released at the interface to the phase change enthalpies of ammonia and water at the absorber pressure. The concentration of the vapor mass absorbed at the interface is different from both the bulk vapor and the vapor concentration at the liquid-vapor interface. Preferential condensation of water out of the vapor typically leads to the lower z than $x_{v,bulk}$ and $x_{v,int}$. This concentration of the condensing flux is used to calculate the mass transfer coefficient using the Colburn and Drew (1937) approach in terms of the molar concentrations. Mass transfer in the liquid phase between the condensing flux at the liquid-vapor interface and the bulk solution is treated as convective rather than diffusive mass transfer, since fluid motion in the liquid phase has a more important role. The convective mass transfer coefficient β_l is determined from the absorbed molar flux and the difference between the molar concentration at the boundary and the average molar concentration of the bulk fluid stream, and converting them to a mass basis. An error propagation method (Taylor and Kuyatt 1994) is used to estimate uncertainties in these heat and mass transfer coefficients. Additional details about these analyses are available in Part I, and in Lee (2007) and Bohra (2007).

2. RESULTS AND DISCUSSION

Solution heat transfer coefficients, and vapor- and liquid-phase mass transfer coefficients are presented here for three absorber pressures, four different dilute solution concentrations, and three different concentrated solution flow rates. In the presentation of the results, the concentrated solution flow rates are shown in terms of the linear mass flux based on the tube length. Thus, the concentrated solution flow rate is divided by the total length of the four tubes over which the solution flows, and further divided by a factor of two to account for the fact that the solution flows around two sides of a tube. This yields a concentrated solution mass flux $\Gamma = \dot{m}/\left(2 \times L_{tube} \times N_{tube}\right)$. Therefore, nominal flow rates of 0.019, 0.026, and 0.034 kg/s correspond to 0.0081, 0.0113, and 0.0146 kg/m-s, respectively.

2.1 Solution Heat Transfer Coefficient

Figure 1 shows the solution heat transfer coefficient for all the data points obtained in the present study, which range from 923 to 2857 W/m^2-K, depending on the test condition. (The trend in the solution heat transfer coefficient was similar to the corresponding trend in the overall U, due to the large absorber coolant heat transfer coefficients for most of the test conditions. By keeping the coolant heat transfer coefficient high, the solution-side resistance becomes dominant and the effect of the coolant-side heat transfer coefficient is minimized, which yields low uncertainties in the absorption heat transfer coefficients. The solution heat transfer coefficient increases with the solution flow rate, and in general, decreased with an increase in P_{abs} and x_{Dilute}. At 150 kPa, at a given concentrated solution flow rate, the solution heat transfer coefficient decreases with increasing dilute solution concentration. Solution heat transfer coefficients are the highest for the 5% nominal concentration case. At a nominal concentration of 40%, the heat transfer coefficients are lower than those for 5% and 15% for all flow rates. The low absorber pressures of 150 kPa necessitate the use of the subcooler described in the previous section for solution concentrations of 15%, 25% and 40%. This results in some of the sensible heat being removed prior to the solution entering the absorber, which reduces absorber heat duties and could cause a decrease in the solution heat transfer coefficient. In other words, the sensible heat fraction in the 5% nominal solution concentration case is larger (because the subcooler is not used) compared to the data at the other concentrations, leading to larger absorber heat duties. It should also be

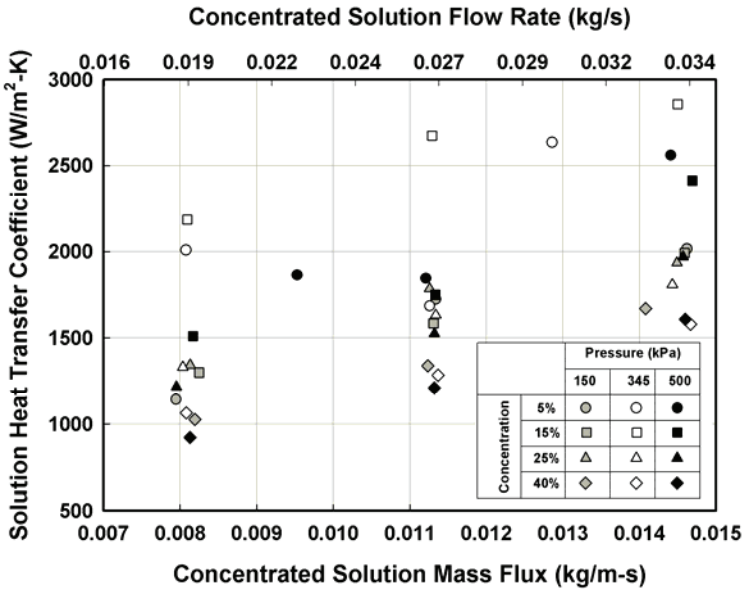

Figure 1. Solution Heat Transfer Coefficient

noted that due to the challenges in testing described above, the nominal combination of low pressure (150 kPa) and high concentration (40%) was in reality tested at somewhat higher absorber inlet pressures (241 – 276 kPa, depending upon the flow rate). These different actual pressures for the same nominal pressure could also contribute to some of the differences in heat transfer coefficients, and therefore the trends seen in Figure 1 represent the combined influence of changes in concentration as well as operating pressure. At 345 kPa, the 5%, and 15% concentration cases show higher heat transfer coefficients than those for the 25%, and 40% nominal concentrations, mostly due to the larger concentration range at the absorber. The lowest solution heat transfer coefficients are observed for the 40% dilute solution concentration case. At 500 kPa, at low flow rates, the solution heat transfer coefficients for the 25% and 40% are lower than those of 5%, and 15%. The 5% and 15% nominal concentration cases required very low coolant flow rates to maintain the higher absorber pressures, which resulted in very large coolant ΔTs. To keep the coolant temperature difference within reasonable limits, the coolant inlet temperature is increased by using a cartridge heater in the absorber coolant loop, which resulted in different driving temperature difference profiles along the absorber. This may have affected the absorption rates and heat transfer coefficients. The heat transfer coefficients for 40% concentration are in general the lowest, which may be because of the smaller driving concentration gradients available for absorption into the solution richer in ammonia. Thus, Figure 1 represents the combined influence of changes in solution flow rate, concentration, and operating pressure. The combined dependence of absorber performance on operating conditions also indicates the differences between a complete absorption system and a component test facility where a greater control over conditions can be obtained.

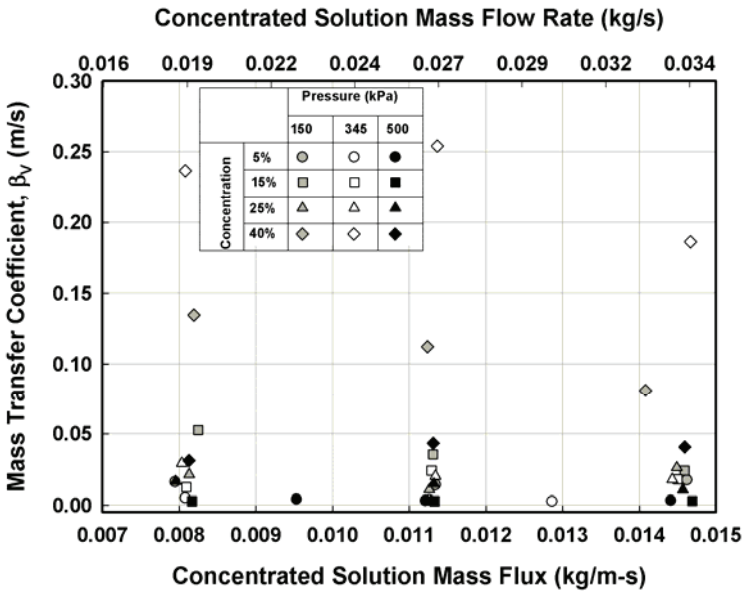

Figure 2. Vapor-Phase Mass Transfer Coefficient

2.2 Vapor-Phase Mass Transfer Coefficient

Figure 2 shows the variation of the overall mass transfer coefficient in the absorber with concentrated solution flow rate. For the range of experiments conducted, the mass transfer coefficient varies between 0.0025 m/s and 0.26 m/s with the uncertainties in the range of 4.6 - 14.2%, depending upon the operating condition. The highest mass transfer coefficient is observed for 40% at 345 kPa, while the smallest value is observed for 15% at 500 kPa. It is found that higher mass transfer coefficients at any pressure are obtained as the dilute solution concentration increases. In general, the vapor-phase mass transfer coefficient is found to decrease with increasing pressure. However, except for the 40% concentration cases, the variation in vapor-phase mass transfer coefficient with pressure is very small. In addition, the variation of vapor-phase mass transfer coefficient with solution concentration also decreases as the absorber pressure increases. As noted before, it was necessary to use different inlet conditions and driving potential differences to achieve these vastly different test conditions. Differences in coolant flow rates, coolant temperatures, degree of sub-cooling, and refrigerant mass flow rates all contribute simultaneously to these changes in mass transfer coefficient. It is also found that the vapor-phase mass transfer coefficient is not very sensitive to the concentrated solution flow rate. This trend is different from that for the heat transfer coefficient, where the heat transfer coefficient increases monotonously with an increase in concentrated solution flow rate. The relative insensitivity of the vapor-phase mass transfer coefficient to the solution flow rate implies that the mass transfer process is governed by the vapor-phase mass transfer resistance. Since in the present study, the vapor phase is quiescent, the large vapor-phase mass transfer resistance should not be influenced by the liquid-phase flow rate.

2.3 Liquid-Phase Mass Transfer Coefficient

Figure 3 shows the variation of the overall mass transfer coefficient in the liquid phase. Effects of pressure and concentration can be seen in this figure; however, the concentrated solution flow rate does not appreciably affect the

mass transfer coefficients in the liquid-phase except for the cases with a pressure of 500 kPa and a concentration of 40%. For the conditions investigated, the liquid-phase mass transfer coefficient varies between 5.51×10^{-6} m/s and 3.31×10^{-5} m/s. The highest mass transfer coefficient is observed for 40% at 500 kPa, while the smallest value is observed for 25% at 150 kPa. It is found that the liquid-phase mass transfer coefficient increases with an increase in concentration at high pressures (e.g., 500 kPa). The lower liquid-phase mass transfer coefficients at the absorber pressure of 150 kPa and dilute solution concentrations of 25% and 40% could be due to the use of a sub-cooler to obtain these conditions. In addition, the 40% cases could only be tested at a pressure of 240 kPa, which is higher than the nominal pressure of 150 kPa. Absorber pressure appears to be an important parameter in determining liquid-phase mass transfer coefficient at all concentrations except 5%. From these trends, it appears that the mass transfer process is governed by the transport properties in the liquid phase, since concentration and pressure affect the mass transfer coefficient in the liquid phase more than the solution flow rate does. Changes in viscosity and binary diffusion coefficient were found to be more prominent than those in the other properties with the variation of concentration and absorber pressure. For example, at an absorber pressure of 345 kPa and a concentrated solution flow rate of 0.026 kg/s, with an increase in concentration from 5% to 40%, the viscosity increases from 3.8×10^{-4} to 9.65×10^{-4} kg/m-s, and the diffusion coefficient decreases from 7.34×10^{-9} to 3.54×10^{-9} m^2/s, while the mass transfer coefficient in the liquid phase increases from 1.53×10^{-5} to 2.58×10^{-5} m/s. At a constant dilute solution concentration of 15% and concentrated solution flow rate of 0.034 kg/s, with an increase in absorber pressure from 150 to 500 kPa, the viscosity decreases from 0.826×10^{-3} to 0.344×10^{-3} kg/m-s, while the diffusion coefficient increases from 3.98×10^{-9} to 7.86×10^{-9} m^2/s and the liquid mass transfer coefficient decreases from 1.65×10^{-5} to 1.38×10^{-5} m/s.

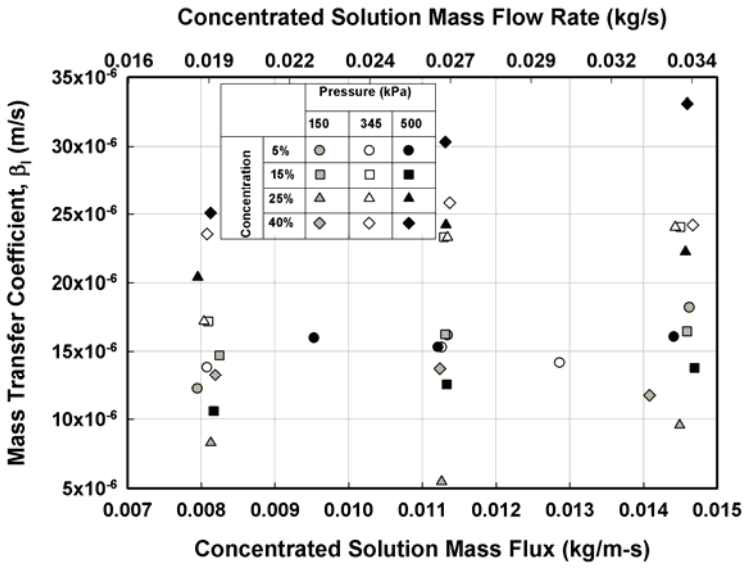

Figure 3. Liquid-Phase Mass Transfer Coefficient

3. COMPARISON WITH THE LITERATURE

There are very few studies in the literature that provide correlations for Nu_l in the horizontal tube falling-film configuration for ammonia-water absorption. The available correlations with any relevance to the present study are used here for comparison with the present data. It should be noted that these studies use different definitions for some of the parameters such as the solution *Re*, mass flux and the film thickness. The differences in these definitions were appropriately accounted for while using these correlations to predict the present data. To avoid confusion due to the different definitions, the falling-film heat transfer coefficients from this study, rather than the Nusselt numbers, are compared with the predictions from the literature.

Figure 4 shows a comparison of the heat transfer coefficients obtained in the present study with the predictions from Wilke (1962), Dorokhov and Bochagov (1983), Hu and Jacobi (1996), Kwon and Jeong (2004), and the data of Meacham and Garimella (2002; 2004). It should be noted that none of these correlations was developed for a falling-film tube absorber in an ammonia-water system (except for the data of Meacham and Garimella, which were on horizontal tube banks with tubes of 1.575 mm O.D.). It can be seen that Wilke (1962) correlation for the flow of water-glycol over a vertical tube (42 mm O.D., 2.4 m long) for different ranges of the solution Reynolds number ($Re_l < 400$; $400 < Re_l < 800$; $Re_l > 800$) shows reasonable agreement with the present data. The disagreement between his predictions and the present data may be due to the differences in geometry and the range of *Re*. For most of the data from the present study, the solution *Re* is less than 100. Also, his study did not involve any gas absorption and was simply a study of single-phase heat transfer in a falling film. The Dorokhov and Bochagov (1983) correlation for the flow of 57% $LiBr/H_2O$ over a column of six horizontal tubes predicts much higher values of heat transfer coefficients compared to the data from the present study. The disagreement may be due to the very

small absorber pressures (~10 kPa) characteristic of LiBr-H_2O systems and the higher solution mass flux in their study, and also because LiBr-H_2O is a fluid pair with a non-volatile absorbent whereas NH_3-H_2O has a volatile absorbent. Their solution mass flux varies between 0.05 and 0.25 kg/m-s, which is significantly higher than the highest mass flux (0.015 kg/m-s) in the present study. In addition, their correlation is valid for $1 < 2 \cdot Pe_l \cdot \delta_l / (\pi \cdot d) < 20$; and the data from the present study are towards the lower limit ($2 \cdot Pe_l \cdot \delta_l / (\pi \cdot d) \sim 1$) of the validity of their correlation. The Hu and Jacobi (1996) correlation for falling films of Water/Glycol mixture and other fluids on a horizontal tube with droplet mode flow between tubes also predicts higher heat transfer coefficients for the range of conditions tested in the present study. The higher predictions of the heat transfer coefficient may be due to the different film thickness definition $\delta = \left(\nu^2 / g\right)^{1/3}$ used by them, which makes the film thickness independent of the solution flow rate. In addition, their correlation does not account for gas absorption and is only for single-phase heat transfer in films falling around horizontal tubes. The Kwon and Jeong (2004) correlation for ammonia/water absorption on a 12.7 mm tube helical coil absorber with a coiling diameter of 82.7 mm based on solution Re and liquid-vapor interfacial shear stress ratio predicts much smaller solution heat transfer coefficients than the present values. This may be due to the different driving temperature differences used in the two studies. Their solution temperatures are close to saturation temperatures corresponding to the absorber pressure and solution concentrations in their study, while the solution is considerably subcooled in the present study. The disagreement is more pronounced for the extreme concentration conditions (5% and 40%). This is probably due to the higher uncertainty reported by them for the lower concentration cases, and the limited applicability at dilute solution concentrations higher than 30% (as the highest dilute solution concentration is 30% in their study). In addition, the absorber pressures are also low (17 - 193 kPa) in their study compared to the range 170 – 520 kPa in the present study. The results of Meacham and Garimella (2002) for NH_3/H_2O absorption on a falling-film absorber consisting of 1.575 mm O.D. microchannels in a square array are corrected for the difference in *LMTD* definitions in the two studies and plotted in Figure 4. Their solution mass flux varied in the range 0.0014–0.0053 kg/m-s and the vapor concentration varied in the range 5 – 50%. Their data show much smaller experimental heat transfer coefficients; however, it should be kept in mind that the mass fluxes in their study are much smaller than those in the present study. This is because, although the mass flow rates used by them were similar (0.010 to 0.040 kg/s) to those in the present study (0.019-0.034 kg/s), the solution was distributed over 27 microchannel tubes, 0.140 m long for a total length of 3.78 m, whereas in the present study the total tube length per row was 1.17 m. The data of Meacham and Garimella (2004) show much higher film heat transfer coefficients compared to the results from their previous study (Meacham and Garimella 2002). The increase was attributed to significant improvement in the solution distribution over the tube array. It can also be seen that their newer data have heat transfer coefficients comparable to those from the present study even at much smaller solution mass fluxes. The differences between their experimental values and the present data may be due to the microchannel geometry used by them.

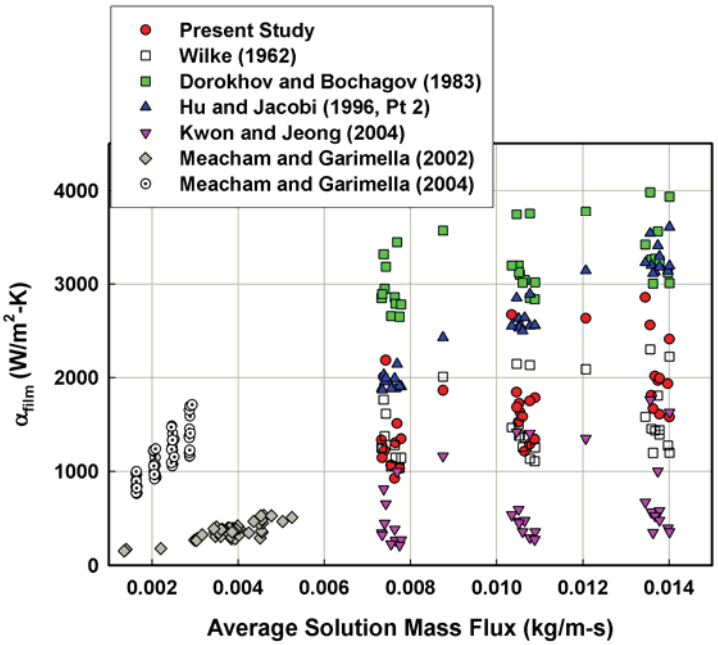

Figure 4. Comparison of Solution Heat Transfer Coefficients with the Literature

There are again few studies in the literature that provide correlations for mass transfer in ammonia-water absorption. The mass transfer coefficients from this study are therefore compared with those obtained using a heat and mass transfer analogy and these reported by Onda *et al.* (1968). In general, the heat and mass transfer analogy is used to address the coupled heat and mass transfer process in analytical studies. However, the use of the heat and mass transfer analogy and correlations from the literature require the vapor-phase heat transfer coefficient, which in turn

requires a vapor-phase Reynolds number (Re_v). Although due to the large absorption chamber occupied by the vapor in this study, no obvious definition of Re_v emerges, for the purpose of comparison, $Re_{v,max}$ for the present study is defined based on the minimum flow area in the tube array along the solution flow path. The vapor-phase $Sh_v = \beta_v \cdot d_{o,t} / D_{aw,v} = Nu_v \cdot \left(Sc_v / \mathrm{Pr}_v\right)^{1/3}$ is calculated from the heat and mass transfer analogy, where the heat transfer coefficient is estimated using the correlation of Churchill and Bernstein (1977) for cross flow over cylinders. The Onda *et al.* (1968) correlation was developed for mass transfer coefficient between gas and liquid phases in packed columns during gas absorption and desorption. The packed column used various random packing, such as Raschig rings and Berl Saddels, with a nominal size of 6 – 50 mm. The liquid-side mass transfer correlation was developed for gas absorption and desorption with water and organic solvents such as methanol and carbon tetrachloride, while the gas-side mass transfer correlation was developed for gas absorption and vaporization with an air-water system. Again, solely for the purpose of comparison, the tube array under consideration is approximated to be analogous to the metal Raschig rings investigated by Onda *et al.* (1968). Thus, $Sh_v = \beta_v / D_{aw,v} \cdot a = 2.0 \cdot \left(a \cdot d_{o,t}\right)^{-2.0} \cdot \mathrm{Re}_{effective,v}^{\ 0.7} \cdot \mathrm{Pr}_v^{1/3}$ where a (m^2/m^3) is the inverse of the characteristic length of the packing. The characteristic lengths for various commercial packings is tabulated in Mills (1995) for different sizes. From these values, the characteristic length was approximated using a curve-fit for the tube size of the present study. Figure 5 shows a comparison of β_v obtained from the data, the heat and mass transfer analogy, and from the correlation of Onda *et al.* (1968). The mass transfer coefficients from the heat and mass transfer analogy and Onda *et al.* (1968) are significantly lower compared with the data from present study. The discrepancies may be due to an inadequate definition of Re_v for the sake of comparison, because the vapor is essentially deemed to be quiescent in the present study. The predictions of Onda *et al.* (1968) can also differ from the data from the present study due to differences in geometry and the fluids investigated in their study. It is also seen that the predicted mass transfer coefficients are relatively similar for all the data and do not show appreciable effects of absorber pressure or dilute solution concentration.

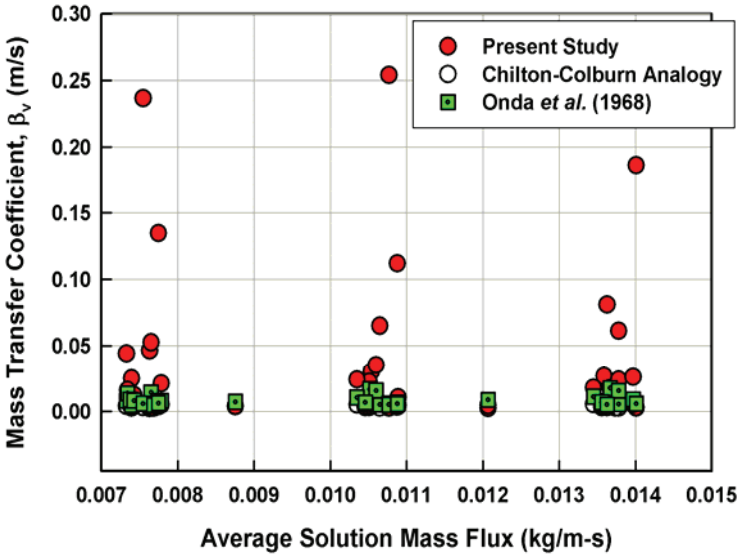

Figure 5. Comparison of Vapor Mass Transfer Coefficients with the Literature

Since there are few studies in the literature that provide correlations for convective mass transfer coefficient in the liquid-phase, the mass transfer coefficients from this study are compared with those obtained using a heat and mass transfer analogy, and with a correlation developed by Inoue *et al.* (2004). The heat and mass transfer analogy in the liquid-phase can be written as $Sh_l = \beta_L \cdot \delta_{film} / D_{aw,l} = Nu_l \cdot \left(Sc_l / \mathrm{Pr}_l\right)^{1/3}$, where β_L is the mass transfer coefficient in the liquid-phase, and δ_{film} is the film-thickness used in the Nusselt number Nu_l. The Inoue *et al.* (2004) heat and mass transfer correlations were for absorption of pure ammonia into falling liquid films formed by distilled water on 17.3 mm horizontal tubes in a steel shell at 11.2-14.7 kPa. Heat transfer coefficients were correlated with the liquid Reynolds number and a temperature ratio (the ratio of temperature differences between the solution inlet and the tube wall, and between the vapor temperature and the tube wall temperature). Mass transfer coefficients in the vapor-phase were correlated with the Schmidt number and Reynolds number of the vapor phase and the ratio of the density of the vapor at the interface and the bulk vapor. Although they developed a heat transfer correlation for the liquid phase and a mass transfer correlation for the vapor phase, they were not compared with the results from the present study, because these correlations of Inoue *et al.* (2004) were expressed in terms of the wall temperature and the vapor-phase Reynolds number, which would be inapplicable for the present study, because a quasi-quiescent vapor here. Inoue *et al.* (2004) did report a correlation for the mass transfer coefficient in the liquid phase in terms

of *Re* and the liquid-phase Schmidt number $Sh_l = \beta_L \cdot \delta_l / D_{aw,l} = 0.26 \cdot \mathrm{Re}_l^{-0.09} Sc_l^{0.005}$, where $\delta_l = \left(\nu_l^2 / g\right)^{1/3}$. Figure 6 shows a comparison of β_L obtained in the present study, the heat and mass transfer analogy, and from the correlation of Inoue *et al.* (2004). Mass transfer coefficients from the heat and mass transfer analogy are higher than the data from the present study. The deviations in the mass transfer coefficient predicted by the analogy and the data from the present study increase as the flow rate increases. This is because the mass transfer coefficients from the present study did not increase proportionately with an increase in Nusselt number, while the mass transfer coefficient predicted by the analogy does so. This implies that mass transfer coefficients were not affected significantly by an increase in the solution flow rate, although the Nusselt numbers are affected by the solution mass flow rate. Values predicted by the correlation of Inoue *et al.* (2004) show somewhat better agreement with the results from the present study, and in general, over predict the current data to some extent. Also, the predictions of Inoue *et al.* (2004) show a greater scatter at a given flow rate than the data from the present study. This scatter may be attributed to differences in the test conditions used by Inoue *et al.* (2004) and the present study. Tests by Inoue *et al.* (2004) were conducted at a single pressure without a change in solution concentration; however, tests for the present study were conducted at three different pressures and four different dilute solution concentrations.

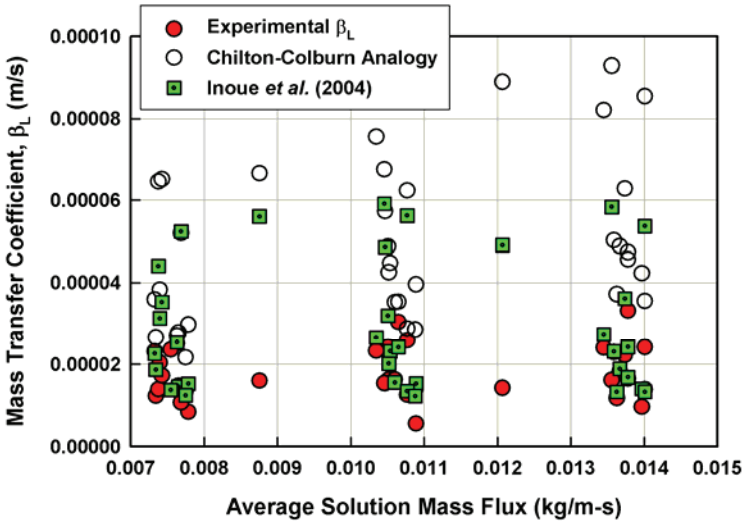

Figure 6. Comparison of Liquid Mass Transfer Coefficient with the Literature

4. CONCLUSIONS

An experimental investigation of ammonia-water absorption heat and mass transfer in a horizontal-tube falling-film absorber was conducted. The experiments over a wide range of concentration, absorber pressure and solution flow rates cover all postulated absorption system operating modes such as refrigeration, air-conditioning, warm-ambient heat pumping, and cold-ambient heat pumping. A facility that allowed measurements of fundamental phenomena such as heat and mass transfer coefficients in a specific component (the absorber) while a full scale absorption system was operating over a wide range of operating conditions was developed and described in Part I of this two-part paper. Such a study that attempts to understand component level heat and mass transfer in a complete ammonia-water absorption heat pump over realistic operating conditions has not been conducted before. Measured quantities such as temperatures, pressures and flow rates at numerous locations around the test loop were analyzed to obtain absorber heat duties, overall and solution heat transfer coefficients, and mass transfer coefficients in the vapor and liquid phases. For the range of experiments conducted, the solution heat transfer coefficient varied from 923 to 2857 W/m^2-K, the mass transfer coefficient in the vapor phase varied from 0.0026 to 0.25 m/s, and the mass transfer coefficient in the liquid phase varied from 5.51×10^{-6} to 3.31×10^{-5} m/s. The solution heat transfer coefficient was found to increase with increasing solution flow rate. In general, the solution heat transfer coefficient was found to decrease with increasing pressure and dilute solution concentration at a given solution flow rate. The mass transfer coefficient showed little effect of the solution flow rate; instead, it is found to be primarily determined by the operating conditions (that affect both the solution and vapor properties). The studies that addressed somewhat similar geometries or processes reported correlations that did not adequately represent the present data. The present study was conducted only on tubes of a specific diameter (9.5 mm) with a specific transverse (30.6 mm) and longitudinal (20.1 mm) pitch. This study should be extended to tubes of different diameters and pitches to increase the range of applicability of the results. At the fundamental level, the findings of the present study, and the underlying modeling of the flow phenomena would be further aided by detailed investigations on a single tube to understand the evolution of the falling film, the formation of droplets, etc., and the resulting species concentration profiles in ammonia-water absorbers. These studies should be conducted using computational techniques as well as

localized measurements of solution temperatures at different transverse and circumferential locations within the liquid film and along the tube length. Such studies would assist in strengthening the hydrodynamic bases used for the correlations developed in the present study. Finally, similar studies on other fluid pairs with volatile and nonvolatile absorbents would assist in the understanding of coupled heat and mass transfer processes in space-conditioning, chemical processing, waste heat recovery, and other diverse applications.

NOMENCLATURE

A	Area (m^2)
LMTD	Log Mean Temperature Difference
P	Pressure (kPa)
Q	Heat Duty (kW)
U	Overall heat transfer coefficient (W/m^2-K)
x	Mass concentration
z	Mass concentration of condensing flux

Greek Symbols

α	Heat transfer coefficient (W/m^2-K)
β	Mass transfer coefficient (m/s)
$\dot{\Gamma}$	Mass flow rate per unit length per side of tube (kg/m-s)

Subscripts

int	Interface
l	Liquid/solution
OD	Outer diameter
v	Vapor

ACKNOWLEDGEMENT

The authors would like to acknowledge support for this research from the Air-Conditioning and Refrigeration Technology Institute and the US Department of Energy (ARTI 21CR Program Contract Number 612-10050.)

REFERENCES

Beutler, A., Ziegler, F. and Alefeld, G. (1996), "Falling Film Absorption with Solutions of a Hydroxide Mixture," *International Ab-Sorption Heat Pump Conference*, Montreal, Canada, pp. 303-309.

Bohra, L. K. (2007). "Analysis of Binary Fluid Heat and Mass Transfer in Ammonia-Water Absorption," Ph.D., Mechanical Engineering, Georgia Institute of Technology, Atlanta, GA.

Churchill, S. W. and Bernstein, M. (1977), "Correlating Equation for Forced Convection from Gases and Liquids to a Circular Cylinder in Crossflow," *Journal of Heat Transfer, Transactions ASME*, **99 Ser C** (2): 300-306.

Colburn, A. P. and Drew, T. B. (1937), "The Condensation of Mixed Vapours," *AIChE Transactions*, **33**: 197-212.

Dorokhov, A. R. and Bochagov, V. N. (1983), "Heat Transfer to a Film Falling over Horizontal Cylinders," *Heat Transfer - Soviet Research*, **15** (2): 96-101.

Hu, X. and Jacobi, A. M. (1996), "The intertube falling film. II. Mode effects on sensible heat transfer to a falling liquid film," *Transactions of the ASME. Journal of Heat Transfer*, **118** (3): 626-33.

Inoue, N., Yabuuchi, H., Goto, M. and Koyama, S. (2004), "Heat and mass transfer of ammonia gas absorption into falling liquid film on a horizontal tube," *Transactions of the Japan Society of Refrigerating and Air Conditioning Engineers*, **21** (4): 299-308.

Killion, J. D. and Garimella, S. (2001), "A critical review of models of coupled heat and mass transfer in falling-film absorption," *International Journal of Refrigeration*, **24** (8): 755-797.

Killion, J. D. and Garimella, S. (2003a), "Gravity-driven flow of liquid films and droplets in horizontal tube banks," *International Journal of Refrigeration*, **26** (5): 516-526.

Killion, J. D. and Garimella, S. (2003b), "A review of experimental investigations of absorption of water vapor in liquid films falling over horizontal tubes," *HVAC and R Research*, **9** (2): 111-136.

Kwon, K. and Jeong, S. (2004), "Effect of vapor flow on the falling-film heat and mass transfer of the ammonia/water absorber," *International Journal of Refrigeration*, **27** (8): 955-964.

Lee, S. (2007). "Development of Techniques for In-Situ Measurement of Heat and Mass Transfer in Ammonia-Water Absorption Systems," Ph.D, Mechanical Engineering, Georgia Institute of Technology, Atlanta, GA.

Meacham, J. M. and Garimella, S. (2002), "Experimental Demonstration of a Prototype Microchannel Absorber for Space-Conditioning Systems," *International Sorption Heat Pump Conference*, Shanghai, China, pp. 270-276.

Meacham, J. M. and Garimella, S. (2004), "Ammonia-water absorption heat and mass transfer in microchannel absorbers with visual confirmation," *ASHRAE Transactions*, **110** (1): 525-532.

Mills, A. F. (1995). Heat and Mass Transfer, Concord, MA, Richard D. Irwin, Inc.

Onda, K., Takeuchi, H. and Okumoto, Y. (1968), "Mass Transfer Coefficients between Gas and Liquid Phases in Packed Columns," *Journal of Chemical Engineering of Japan*, **1** (1): 56-62.

Taylor, B. N. and Kuyatt, C. E. (1994). Guidelines for Evaluating and Expressing the Uncertainty of NIST Measurement Results, National Institute of Standards and Technology.

Wilke, W. (1962), "Heat transfer to falling liquid films (Waermeuebergang an Rieselfilme)," *VDI -- Forschungsheft* (490): 36.